Journal of Catalysis 276 (2010) 402–411

Contents lists available at ScienceDirect

Journal of Catalysis

journal homepage: www.elsevier.com/locate/jcat

Mechanistic aspects of the selective catalytic reduction of NO_x by dimethyl ether and methanol over γ-Al_2O_3

Stefanie Tamm *, Hanna H. Ingelsten, Magnus Skoglundh, Anders E.C. Palmqvist

Competence Centre for Catalysis, Chalmers University of Technology, SE-412 96 Göteborg, Sweden
Applied Surface Chemistry, Chalmers University of Technology, SE-412 96 Göteborg, Sweden

ARTICLE INFO

Article history:
Received 10 May 2010
Revised 6 October 2010
Accepted 7 October 2010
Available online 9 November 2010

Keywords:
DME
Methanol
γ-Al_2O_3
SCR
deNO_x
Reaction mechanism
DRIFT spectroscopy

ABSTRACT

High catalytic activity for selective catalytic reduction of NO_x with dimethyl ether and methanol (DME- and methanol-SCR) has been found over a γ-alumina catalyst. The surface species involved in the DME-SCR reaction were studied by diffuse reflectance infrared Fourier transform spectroscopy (DRIFTS) in combination with mass spectrometry and compared to the corresponding species observed during methanol-SCR. Dimethyl ether adsorbs mainly as methoxy groups (—O—CH_3) on the catalyst surface, while methanol adsorbs as methoxy groups and molecularly. With increasing temperature, DME desorbs in two steps, whereas methanol desorbs first as methanol and at higher temperatures as DME. At higher temperatures, the two reducing agents display similar DRIFTS spectra showing first formaldehyde-like species and then formates on the surface. In the presence of NO or NO_2, reactions between NO_x species and carbon-containing species occur. Formohydroxamic acid (CHO—N(H)OH) forms isocyanates (NCO), and both are observed at temperatures relevant for DME-SCR. Since these species are likely intermediates for hydrocarbon-SCR over Ag/Al_2O_3, a partly similar reaction mechanism may be operational for DME-SCR over γ-Al_2O_3 despite the fact that Ag/Al_2O_3 does not catalyze DME-SCR efficiently. The difference is thus due to the reaction steps leading to the formation of formohydroxamic acid that with DME follow a more efficient route over γ-Al_2O_3 than over Ag/Al_2O_3.

1. Introduction

Dimethyl ether (DME) and methanol are energy efficient and low CO_2 emitting alternative fuels when produced from biomass [1,2]. However, similar to more conventional hydrocarbon-based fuels, combustion of DME or methanol in an engine results in NO_x formation. This harmful emission needs to be reduced in order to fulfill the most stringent upcoming legislation limits for vehicles. One attractive technique to reduce NO_x emissions from vehicle engines is selective catalytic reduction with the fuel, i.e. DME-SCR or methanol-SCR. However, the two currently most widely researched catalysts for hydrocarbon-SCR, Ag/Al_2O_3 and Cu-ZSM-5, have shown very low activity for NO_x reduction with DME and methanol. The NO_x conversion over Cu-ZSM-5 was less than 5% with DME in the presence of water and over Ag/Al_2O_3 less than 30% with DME or methanol and with high selectivity to N_2O [3–5]. This behavior cannot be explained with the widely discussed reaction mechanism for conventional HC-SCR over Ag/Al_2O_3. In this reaction mechanism, it is believed that nitrates, nitrites or NO_x from the gas phase [6–8] reacts with partly oxidized hydrocarbons as for example aldehydes or acetates [6,7,9] via C- and N-containing intermediates [7,10], possibly nitromethane and formohydroxamic acid [11–14] to isocyanates and cyanide species [6–8,10,13,15,16]. These species can then be hydrolyzed to amines or ammonia, which react with nitrates, nitrites or NO_x from the gas phase to form N_2 [6–8,10,13,15,16].

In contrast to Ag/Al_2O_3, comparably high DME- and methanol-SCR activity showing 68–100% NO_x reduction has been reported over pure γ-Al_2O_3, or Al_2O_3 supported base metals such as Mo/Al_2O_3, Sn/Al_2O_3 and Co/Al_2O_3 catalysts with high selectivity to N_2 [17–19] and with activity for NO_x reduction between 250 and 550 °C [5,17–19]. Presently, there are only few studies published aiming at explaining the differences between DME or methanol and more conventional hydrocarbon-based reducing agents in HC-SCR. Recently, we showed that DME is a special reducing agent as it induces gas-phase reactions with O_2 and NO_x at temperatures above 300 °C. These reactions dramatically change the gas composition reaching the catalyst and put additional design criteria on efficient DME-SCR catalysts [20]. A comparison between DME and methanol as reducing agents indicated moreover that these gas-phase reactions boost the NO_x conversion over γ-Al_2O_3 but do not improve the reactions over a Ag/Al_2O_3 catalyst [5].

* Corresponding author. Address: Applied Surface Chemistry, Competence Centre for Catalysis, Department of Chemical and Biological Engineering, Chalmers University of Technology, SE-412 96 Göteborg, Sweden. Fax: +46 (0) 31 16 00 62.
E-mail address: stamm@chalmers.se (S. Tamm).

0021-9517/$ - see front matter © 2010 Elsevier Inc. All rights reserved.
doi:10.1016/j.jcat.2010.10.004

On the surface of γ-Al_2O_3, methoxy groups (—OCH_3) and molecularly adsorbed methanol and DME are suggested to be the main surface species formed upon adsorption of DME at low temperatures, whereas formates dominate at higher temperatures [21]. Sequential adsorption of DME and NO_2 was reported to result in a competition for adsorption sites at 150 °C. A fast reaction between methoxy groups and NO_2 was found to result in formation of isocyanates and formates at 300 °C [21]. In the present study, the surface species on γ-Al_2O_3 relevant for DME- and methanol-SCR are investigated during temperature-programmed desorption and reaction experiments, and their involvement in the DME- and methanol-SCR reaction is discussed. These results are, moreover, compared to the mechanism proposed for conventional hydrocarbons over Ag/Al_2O_3.

2. Materials and methods

A γ-alumina powder sample (SASOL Puralox SBa-200) was used as received. Following a heat treatment at 225 °C in vacuum, the BET surface area of the sample was found to be 176 m^2/g as determined by N_2 sorption at −196 °C using a Micromeritics ASAP 2010.

In situ DRIFT spectroscopy experiments were performed using a BioRad FTS 6000 FTIR spectrometer equipped with a high-temperature reaction cell (Harrick Scientific, Praying Mantis) with KBr windows. The temperature of the reaction cell was controlled with a K-type thermocouple connected to a Eurotherm 2416 temperature controller. Gases were introduced into the reaction cell via individual mass flow controllers, and methanol was introduced by a liquid delivery system with vapor control, consisting of a liquid flow controller, a mass flow controller for carrier gas and a temperature-controlled mixing and evaporation device (all Bronkhorst Hi-Tech). The gas composition at the outlet of the DRIFTS cell was analyzed by mass spectrometry (Balzers QuadStar 420).

Each temperature-programmed desorption (TPD) and temperature-programmed reaction (TPR) experiment were performed using approximately 100 mg of a fresh γ-Al_2O_3 powder sample. For these experiments, the sample was initially pretreated in a flow of 8% O_2 in Ar at 550 °C for 30 min, subsequently cooled to 30 °C in Ar where a background spectrum (60 scans, resolution 2 cm^{-1} at 4000 cm^{-1}) was recorded. In all following experiments, this spectrum was used as background, since it results in the straightest baseline and thus simplifies interpretation of the results. The positions and trends of the developed absorption bands were found not to be affected by the choice of temperature for the recorded background. The evolution of absorption bands in the spectra was followed using the kinetic mode (9 scans/spectrum, 6 spectra/min) at a resolution of 2 cm^{-1} at 4000 cm^{-1}. The data are presented as absorbance, which is defined as the logarithm of the inverse reflectance ($\log 1/R$). In the experiments, dimethyl ether (1000 ppm in Ar) or methanol (1000 ppm in Ar) was adsorbed on the catalyst sample at 30 °C for 30 min. The sample was then flushed with Ar for 30 min which, in some cases, was followed by 15-min exposure to 500 ppm NO or NO_2 in Ar. Thereafter, the temperature was raised (in Ar or in a mixture of Ar and NO_x) with a ramp rate of 10 °C/min to 500 °C. This temperature ramp was interrupted in intervals of 50 °C (at 50 °C, 100 °C, 150 °C, etc.) where the temperature was kept constant for 15 min to approach steady-state conditions for the surface species. Subsequently, the experiment was repeated with the same sample for a second TPD or TPR experiment without interruptions to obtain clear desorption peaks for the gas phase. Since similar gas compositions were observed for both types of temperature ramps (with and without interruptions), only the desorption peaks of the ramps without interruption are presented. All experiments were carried out using a total flow rate of 100 mL/min at 20 °C and atmospheric pressure which corresponds to a space velocity of about 62,000 h^{-1}.

The assignment of the mass-to-charge ratio (m/z) signals from the mass spectrometer to the different species is shown in Table 1. In the absence of N-containing species, an unambiguous assignment of the mass-to-charge ratio to gas species is possible. However, in the presence of NO_x, m/z = 28 represents the sum of CO and N_2. Since the formation of both of these gases has been observed in previous activity tests [5], the assignment is made to CO/N_2. Moreover, m/z = 44 can be due to CO_2 and N_2O. Since only a maximum of 2% N_2O formation was observed in previous activity tests over the same catalyst [5], N_2O formation is less likely also in the present study. Nevertheless, the possibility of N_2O formation is mentioned when NO_x is present, since its formation cannot be ruled out. All mass spectrometer signals were divided by the signal of m/z = 40 (Ar) to compensate for possible pressure changes in the mass spectrometer cell. Moreover, to compensate for the contributions from DME and methanol to m/z = 15, the two products $0.5\cdot(m/z = 45)$ and $0.3\cdot(m/z = 31)$ were subtracted from m/z = 15 to obtain the signal representing CH_4. The mass spectrometer signals for NO and NO_2 (m/z = 30 and 46) are not included in the figures since NO and NO_2 were provided in excess.

3. Results and discussion

The temperature-programmed desorption of DME and the temperature-programmed reaction experiments of DME, in the presence of NO or NO_2, were performed in the DRIFTS cell, where the gas composition at the cell outlet was continuously monitored with mass spectrometry. The experimental setup used allowed for the correlation between gas phase and surface species and facilitated the search for potential intermediates in the DME-SCR reaction over γ-Al_2O_3. Although DME-SCR conditions are characterized by excess oxygen, experiments were performed in both the absence and presence of O_2. In the DME-TPR with NO, a larger number of surface species may be observed due to lower formation of nitrates compared with experiments performed in the presence of O_2. In the presence of O_2, the bands of the nitrates overlap with those of several other species, making their detection more difficult. The effect of the O_2 concentration in the gas mixture on the surface species has not been studied; however, no difference in surface species was observed between experiments performed in the presence or absence of O_2 during the DME-TPD or in the DME-TPR with NO_2. Consequently, this paper focuses on the results from the experiments performed in the absence of oxygen. Results from experiments in the presence of oxygen are available as Supplementary material.

3.1. Temperature-programmed desorption over γ-alumina

Fig. 1a shows the mass spectrometer signals collected during DME-TPD over γ-Al_2O_3 in a flow of Ar. Dimethyl ether desorbs in

Table 1
Assignment of m/z signals measured by mass spectrometry during catalytic reactor tests.

m/z (g mol^{-1} e^{-1})	Species
2	H_2
15	CH_4
18	H_2O
28	CO, N_2
31	H_3COH
40	Ar
44	CO_2(, N_2O)
45	DME

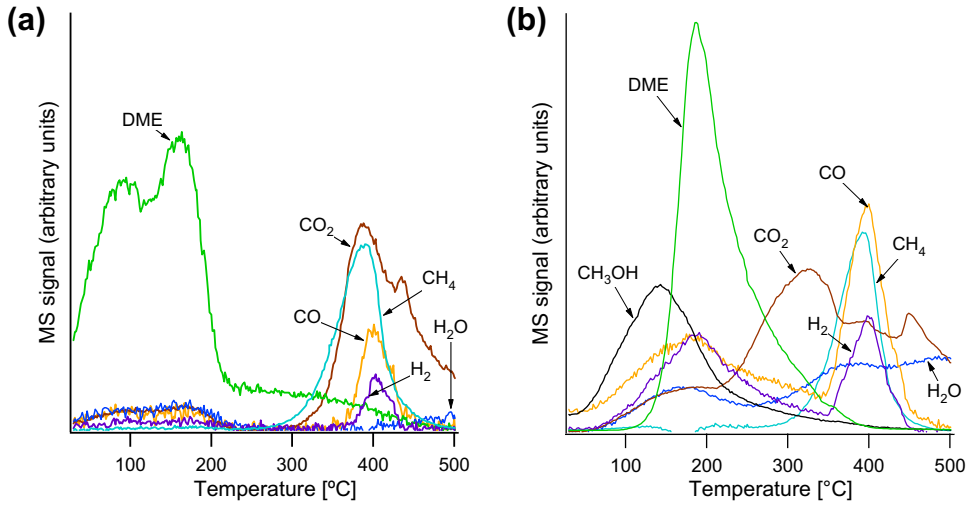

Fig. 1. Temperature-programmed desorption profiles from γ-alumina with pre-adsorbed DME (a) or methanol (b) in an Ar flow.

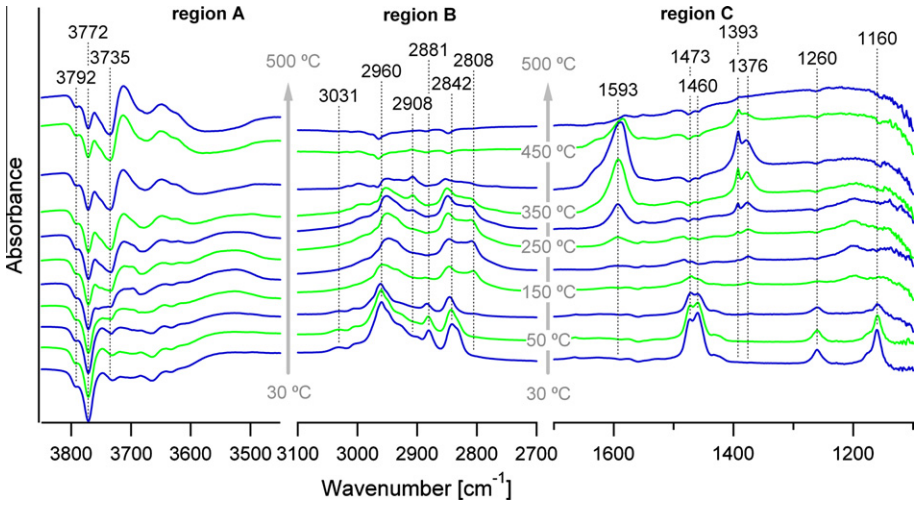

Fig. 2. DRIFTS spectra of γ-alumina samples with pre-adsorbed DME during temperature-programmed desorption in an Ar flow.

two broad peaks between room temperature and 200 °C, together with small amounts of CO, CO_2, H_2O and H_2. Above 300 °C, peaks from desorption of CH_4 and CO_2 arise with maxima around 380 °C. From 350 °C, CO and H_2 desorb and peak around 400 °C. For comparison, Fig. 1b shows the desorption properties from the corresponding methanol-TPD, where methanol starts to desorb directly upon heating from 30 °C and reaches a peak at 140 °C. At a somewhat higher temperature, CO, H_2, CO_2 and H_2O desorb, all with a peak around 190 °C. Also dimethyl ether shows a very sharp desorption peak at this temperature although its desorption commences at a somewhat higher temperature. The subsequent decrease in DME, CO, H_2 and H_2O at higher temperatures is accompanied by a diffuse increase in H_2O and an increase in CO_2, which shows a second peak around 325 °C. Above this temperature, CH_4 desorbs rapidly followed by sharp peaks of CO and H_2 all peaking around 400 °C. These observations are in accordance with previously reported results of methanol-TPD experiments over different alumina catalysts [22,23].

Formation of other species besides DME and methanol during the TPD clearly shows that reactions take place on the alumina surface. This is supported by the DRIFTS spectra of the γ-Al_2O_3 surface exposed to DME presented in Fig. 2. The lowermost spectrum was recorded at 30 °C after adsorbing DME for 30 min and flushing with Ar for 30 min. The following spectra were recorded at increasingly higher temperatures with 50 °C increments from 50 °C to 500 °C. During this DME-TPD, bands evolved in three different regions of the DRIFTS spectra, where region A covers 3850–3450 cm^{-1}, region B 3100–2700 cm^{-1} and region C 1700–1100 cm^{-1}. The positive bands in regions B and C, which arise when adsorbing DME at 30 °C, may all be attributed to different features of methoxy (—O—CH_3) species or molecularly adsorbed DME. Differentiation between the absorption spectra of methoxy groups and molecularly adsorbed DME is difficult due to the similar vibration frequencies for these species. However, based on the study by Chen et al. [24] where the spectra of molecularly adsorbed DME and methoxy groups are directly compared, we assign all the positive bands in regions B and C to different features of methoxy species, as summarized in Table 2. The methoxy bands diminished in region C with increasing temperature, whereas in region B, the bands either decreased or shifted positions when raising the temperature from 30 °C to 150 °C. In region C, new bands appeared at 250 °C, which can be assigned to different vibrations of formate species as summarized in Table 2. These bands reached a maximum at 400 °C and disappeared at 500 °C. In region A, a negative band at

Table 2
Assignment of the absorption bands observed in the DRIFTS measurements during DME-TPD and methanol-TPD.

Wavenumber (cm^{-1})	Surface species	Vibrational modes	References
3792	Hydroxyl	ν(OH)	[25,26,29]
3772	Hydroxyl	ν(OH)	[25,26,29]
3735	Hydroxyl	ν(OH)	[25,26,29]
3684	Hydroxyl	ν(OH)	[26,29]
3200	Methanol	ν(OH)	[29]
3031	Methoxy	$\nu_{as}(CH_3)$	[24]
2960	Methoxy	$\nu_{as}(CH_3)$	[24,29]
2946–2941	Methoxy or methanol	$\nu_s(CH_3)$	[23,29]
2908	Formate	ν(CH)	[9,51,52]
2881	Methoxy	$\delta(CH_3)$	[24]
2846–2842	Methoxy	$\nu_s(CH_3)$	[24,29]
2821	Methoxy or methanol	$\nu_s(CH_3)$	[23,29]
1593	Formate	ν_{as}(COO)	[9,51–53]
1473, 1460–1455	Methoxy	$\delta_{as}(CH_3)$	[21,24,29]
1393	Formate	δ(CH)	[7–9,51–54]
1376	Formate	ν_s(COO)	[7–9,51–54]
1260	Methoxy	$\gamma(CH_3)$	[24]
1160	Methoxy	$\gamma(CH_3)$	[24]

3772 cm^{-1}, with a shoulder at 3792 cm^{-1}, occurred during DME adsorption at 30 °C. These bands are indicative of the disappearance of free hydroxyl groups from the alumina surface [25,26]. In parallel, a broad positive band is seen between 3600 and 3500 cm^{-1} caused by hydrogen-bonded hydroxyl groups on alumina [25,27,28]. When increasing the temperature, the negative bands were stable within the entire temperature interval studied, showing that the surface remained dehydroxylated during the process. At 250 °C, another negative band developed at 3735 cm^{-1} and became more distinct and deeper with increasing temperature. This band can also be assigned to removal of free hydroxyl groups on the alumina surface [25,26].

The corresponding DRIFTS spectra of the alumina surface with adsorbed methanol are shown in Fig. 3, and the features in the lowermost spectrum can be assigned to methoxy groups and/or molecularly bound methanol as presented in Table 2. The bands due to methanol adsorption are located at slightly different positions than those due to DME adsorption, and thus the surface species appear to be somewhat differently bound in the two cases. Distinct from the adsorption of DME, methanol adsorption showed a broad band around 3200 cm^{-1} below 100 °C (not shown). This band is due to the hydroxyl group of molecularly adsorbed methanol [29,30]. In region C, the bands at 1473 cm^{-1} and around 1457 cm^{-1} are much smaller but broader compared with the case with adsorption of DME. The shape of these bands is in accordance with previous studies of methanol adsorption on alumina [23,24,29–31]. In region A, negative bands of perturbed free OH-groups appear at 3792 and 3772 cm^{-1} similar to those obtained for DME adsorption. However, the negative OH-band at 3735 cm^{-1} was developed already at 30 °C, and an additional negative band at 3684 cm^{-1} was also visible. Moreover, the broad band between 3600 and 3500 cm^{-1}, assigned to hydrogen-bonded hydroxyl groups, is more pronounced. When heating the sample, the bands in region B decreased in intensity and shifted in wave number, and a new band at 2808 cm^{-1} appeared at 150 °C. The evolution of this band was also observed during the DME-TPD in this study and was previously reported, but not assigned [21]. Bands slightly above 2800 cm^{-1} have previously been assigned to the symmetric stretching vibration of C—H of methoxy groups [24], formate species [32] and/or an overtone of the C—H bend of formate or methoxy species [23]. Since the band at 2808 cm^{-1} does not appear until the bands of the methoxy species in the TPD have almost disappeared, but before the bands of the formate species appear in region C, it seems likely that the band at 2808 cm^{-1} is due to an intermediate in the formation of formate from methoxy species. In the gas phase, the symmetric C—H stretching vibrations of formic acid (2943 cm^{-1}) and methanol (2844 cm^{-1}) are clearly higher than the corresponding vibration of formaldehyde at 2783 cm^{-1}. For molecularly adsorbed formaldehyde, this vibration is found at 2818 cm^{-1} [33] or 2788 cm^{-1} [34], and for polymerized formaldehyde at 2805 cm^{-1} [33]. Over alumina, all these formaldehyde species were only detected at temperatures lower than those relevant in this work. However, dioxymethylene species ($O—CH_2—O^{2-}$), an adsorbed formaldehyde-like species, has been reported to be an intermediate in the oxidation of methoxy to formate species over other metal oxides at 200 °C and has been considered but not detected as an intermediate over alumina [35]. Over TiO_2 (anatase), dioxymethylene is characterized by strong C—O stretching bands between 1200 and 1000 cm^{-1} and several bands between 2750 and 3000 cm^{-1} [35]. In Figs. 2 and

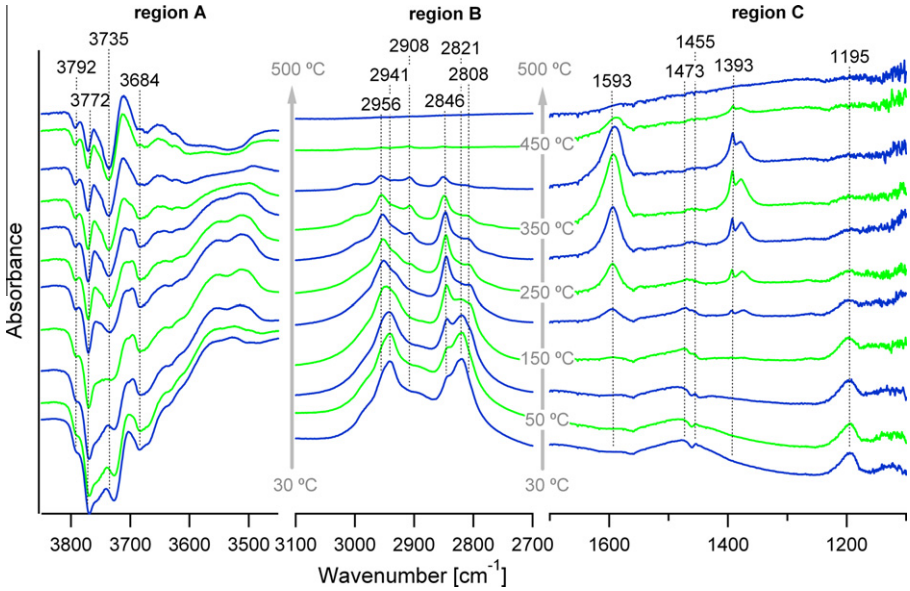

Fig. 3. DRIFTS spectra of γ-alumina samples with pre-adsorbed methanol during temperature-programmed desorption in an Ar flow.

3, there are several bands between 2800 and 3000 cm^{-1}, which can be due to dioxymethylene. Moreover, the broad band between 1240 and 1180 cm^{-1}, observed between 150 and 300 °C, can be due to the C—O stretching of dioxymethylene. Since bands are observed in all regions, where characteristic bands of dioxymethylene occur, we tentatively assign the band at 2808 cm^{-1} to a formaldehyde-like species. The further increase in the temperature led to the formation of formate species similar to the DME-TPD, and above 250 °C the DRIFTS spectra of DME and methanol appear to be identical within the margin of error.

Combining the information obtained from Figs. 1 and 2 allows elaborating more on DME adsorption and desorption on the alumina surface. This is illustrated in black in Scheme 1. When DME adsorbs at room temperature, it mainly reacts with the OH-groups at 3772 cm^{-1} forming methoxy groups and water. When increasing the temperature, DME desorbs in two steps, as indicated by the double peak in Fig. 1a. This double peak indicates the existence of different adsorption sites, possibly different strong Lewis acid sites, as previously proposed for the adsorption of methanol [23]. Below 100 °C, DME desorption is a result of a recombination of two methoxy groups. At 150 °C, very few methoxy groups remain on the surface as indicated by the absence of the methoxy bands in region C in Fig. 2. Above 150 °C, the CH-stretch of a formaldehyde-like species is observed at the same time as free OH-groups on alumina at 3735 cm^{-1} are consumed. The coinciding consumption of OH-groups with the formation of formaldehyde-like species can be explained by a reaction of the OH-groups with methoxy groups forming formaldehyde-like species and H_2 as proposed in the literature [35]. Instead of the proposed formation of H_2, we observe the growth of a broad band between 3600 and 3500 cm^{-1}, which has previously been suggested to be due to hydrogen-bonded surface hydroxyl groups [25,27,28]. At the same temperature, the second desorption peak of DME evolves in the gas phase. At 300 °C, CO_2 and methane are detected in the gas phase, while formates appear and OH-groups are consumed at the surface. The simultaneous detection of methane and CO_2 or formate has been rationalized by the reaction of two methoxy species, while the remaining protons form H_2 and OH-groups are consumed [23]. In contrast, in the present study, all methoxy groups have probably been transformed into formaldehyde-like species at 300 °C. However, the stoichiometry of the reaction between two formaldehyde-like species to methane and CO_2 or formates is consistent with the lack of H_2 formation at that temperature and the decrease in the hydrogen-bonded hydroxyl groups. Hydrogen is detected at a somewhat higher temperature in our experiments and appears together with CO, which has been explained as a result of the decomposition of formates [23]. This appears also to be reasonable in the present study as illustrated in Scheme 1.

Since both DME and methanol adsorption mainly lead to methoxy and methanol species on the alumina surface, their similar TPD behavior shown in Fig. 1 may be expected. The main difference observed is that the first desorption peak in Fig. 1b is due to methanol and not due to DME. This desorption peak coincides with the disappearance of the broad band at 3200 cm^{-1}, indicating desorption of molecularly adsorbed methanol in accordance with previous studies [30]. At 150 °C, the DRIFTS spectra of the DME-TPD and

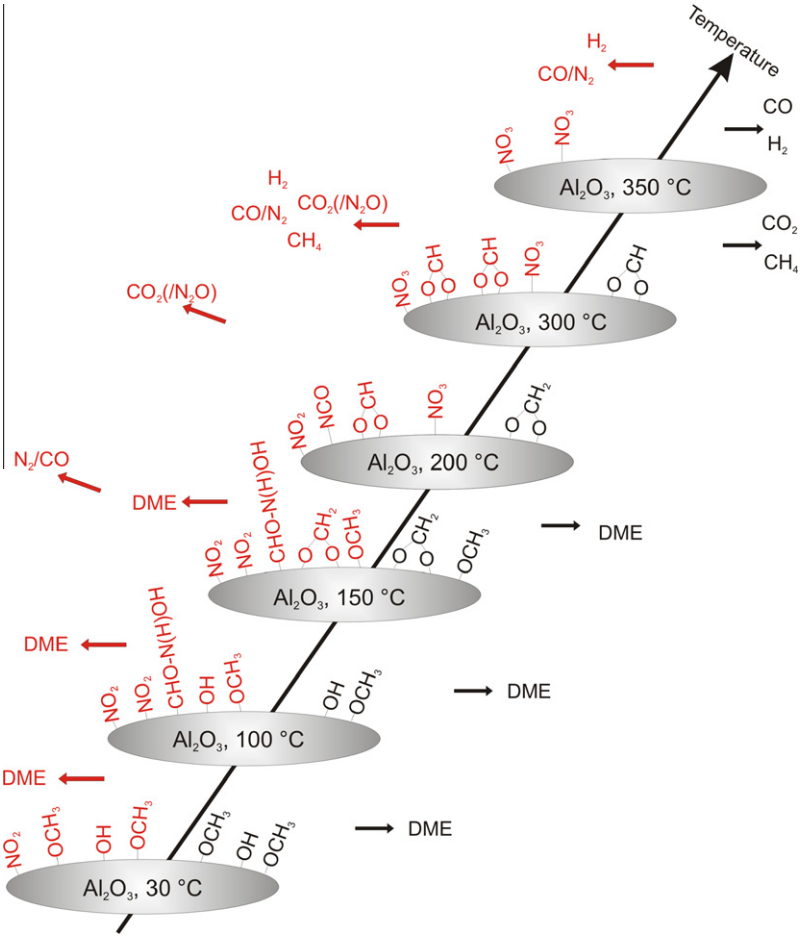

Scheme 1. Possible reaction scheme of the adsorption of DME on γ-Al_2O_3 and subsequent temperature-programmed desorption in an Ar flow (black) or in a flow of 500 ppm NO in Ar (red). (For interpretation of the references to colour in this figure legend, the reader is referred to the web version of this article.)

the methanol-TPD show similar types of features: negative bands in region A, due to consumed free OH-groups; positive bands in region B, due to CH vibrations of methoxy groups; and minor bands in region C. These similarities in surface species at this temperature can explain the DME desorption peak in the methanol-TPD (Fig. 1b), which occurs at almost the same temperature as the second DME desorption peak in the DME-TPD (Fig. 1a). The processes that occur on the catalyst surface at still higher temperatures during the methanol-TPD are likely very similar to those during the DME-TPD, since the DRIFTS spectra are very similar under these conditions. The differences observed are the earlier onset of CO_2 formation in the gas phase and the higher concentration of formed water. They can be explained by the higher oxygen content in methanol compared with DME, which leads to more oxygen available at the surface.

For the experiments performed in the presence of oxygen, the surface species and the reactions on the surface are the same. In the gas phase, however, more CO_2 and methane are formed but less CO and H_2 above 300 °C as shown in the Supplementary material. This may be explained by a preferred reaction of methoxy groups to CO_2 and methane at the expense of the formation of formates. When fewer formates are formed, the decomposition of these generates less CO and H_2.

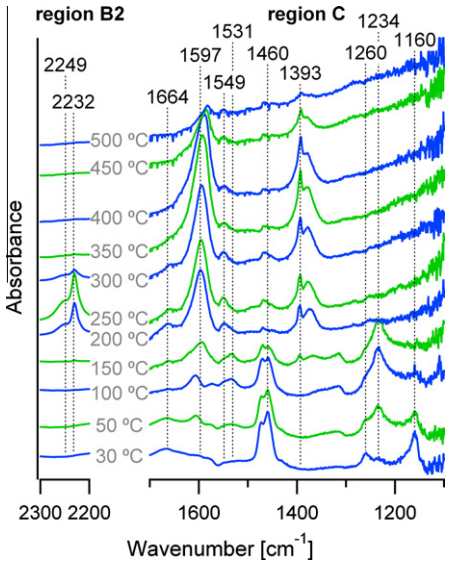

Fig. 5. DRIFTS spectra of γ-alumina samples with pre-adsorbed DME during temperature-programmed reaction in a flow of 500 ppm NO in Ar.

3.2. Reaction of adsorbed surface species with NO

Fig. 4a shows the gases desorbing from γ-Al_2O_3 during the DME-TPR in a flow of 500 ppm NO. Overall, the desorption of gases appears very similar in the presence and absence of NO. Below 200 °C, DME desorbed in a double peak, and above 300 °C, CO_2, CH_4, CO and H_2 are formed. The addition of NO to the gas mixture results in decreased formation of CH_4 but increased formation of H_2 and CO/N_2. Moreover, the formation of CO/N_2 is shifted to lower temperatures. In Fig. 4b, the corresponding results for the methanol-TPR with NO present are shown. Also here, the effect of the addition of NO appears small. Similar to the DME-TPR with NO, the methanol-TPR with NO showed a lower formation of CH_4 in the presence of NO, and the formation peak of CO/N_2 was broader and slightly shifted to lower temperatures compared with the methanol-TPD.

The results of the corresponding DRIFTS measurements for the DME-TPR with NO are shown in Fig. 5. The lowermost spectrum is that of adsorbed DME on alumina at 30 °C and is similar to the lowermost spectrum in Fig. 2. Increasing the temperature results in the same general features as in the DME-TPD: formation of formaldehyde-like species at 150 °C, indicated by the band at 2808 cm^{-1} (not shown in Fig. 5); and formate species at 200 °C, indicated by the band at 1393 cm^{-1}. However, already at 50 °C the presence of NO caused a new band at 1234 cm^{-1}, assigned to nitrite species as summarized in Table 3. Also other features appeared at 200 °C in regions C and B2. The features in region B2 (2249 and 2232 cm^{-1}) can be assigned to isocyanates (NCO) and the bands around 1597 and 1549 cm^{-1} in region C to unresolved vibrations of differently bound nitrates and possibly nitrites as summarized in Table 3.

Between 100 and 150 °C, a band is observed at 1531 cm^{-1}, which previously has been observed in two different studies during TPD of nitromethane (NO_2—CH_3) over γ-alumina where it preceded NCO formation [13,36]. The band at 1531 cm^{-1} was ascribed to a C—N—O-containing precursor of isocyanates, probably formohydroxamic acid (CHO—N(H)OH) [13,36], which is in accordance with the conclusions from other studies [37]. This assignment is also reasonable in the present study.

Similar to the nitrite band at 1234 cm^{-1}, a band at 1664 cm^{-1} is visible already at 30 °C during the DME-TPR in the presence of NO.

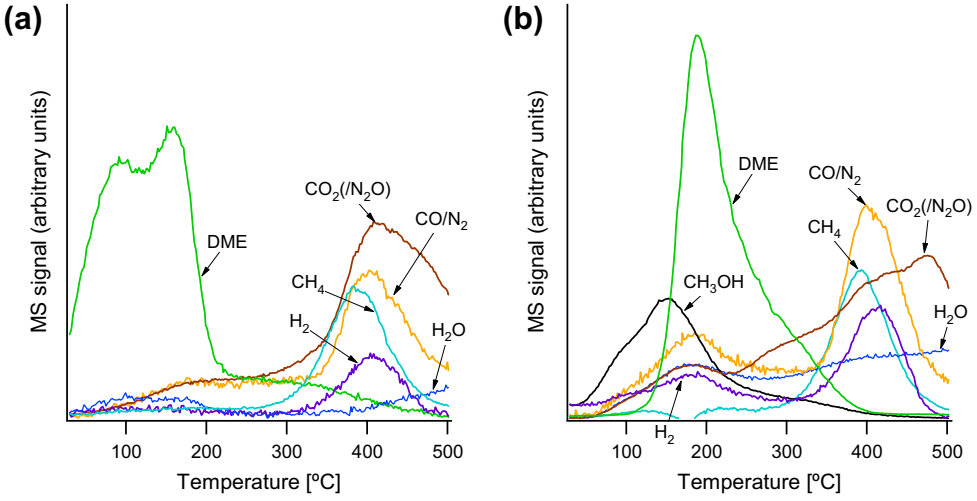

Fig. 4. Temperature-programmed reaction profiles from γ-alumina with pre-adsorbed DME (a) or methanol (b) in a flow of 500 ppm NO in Ar.

Table 3
Assignment of the additional bands observed in the DRIFTS measurements during DME-TPR in the presence of NO_x.

Wavenumber (cm^{-1})	Surface species	Vibrational modes	References
2249	NCO		[8,55]
2232	NCO		[8,55]
1664	R-ONO	ν(N=O)	[10,38–42]
1570–1630	Nitrate and nitrite	ν(N=O)	[9,13,48,49,52,53]
1549	Nitrate	ν(N=O)	[8,13,46,47]
1325	Nitrite	ν_{as}(ONO)	[46,56]
1304	Nitrate	ν_{as}(ONO)	[8,44,49,51,57]
1250	Nitrate	ν_{as}(ONO)	[49,53]
1234	Nitrite	ν_{as}(ONO)	[38,46]

In a separate experiment, a small band at 1664 cm^{-1} was observed during NO-TPD over the same material (results not shown). The assignment of these bands at 1664 cm^{-1} is more ambiguous, as they may be due to the N–O vibration of inorganic or organic nitrites [10,38–40]. Takana et al. reported a considerable difference in the band intensity between inorganic (weak) and organic nitrites (strong) [40]. Since the band at 1664 cm^{-1} increases considerably at 200 °C in Fig. 5, it might be due to organic nitrites above 150 °C. Because there are mainly C_1 compounds on the catalyst surface, it is reasonable to assume that the observed organic nitrites are methyl nitrites (CH_3—ONO). However, in studies with nitromethane (CH_3—NO_2) bands at 1660 cm^{-1} are reported to contain a C—N double bond as nitrosoaldehyde dianion (HC(O)=NO^{2-}), which is discussed as a precursor for NCO species [36,41,42]. Since the band increases and disappears at the same temperatures as the NCO band, an assignment of the band at 1664 cm^{-1} to a nitrosoaldehyde dianion appears also possible. Therefore, the assignment of the band at 1664 cm^{-1} remains ambiguous in this study.

In Scheme 1, the reactions that occur on the catalyst surface during the TPR in the presence of NO are illustrated in red. Below 200 °C, the desorption peaks of DME are quite similar in the presence or absence of NO, because methoxy groups recombine and desorb as DME from the surface. At the same time, nitrites were formed, and the concentrations of CO_2(/N_2O) (m/z = 44) and CO/N_2 (m/z = 28) increased in the presence of NO between 100 and 400 °C. This increased desorption may be caused by a replacement of methoxy groups by NO_x species as previously suggested [21]. Moreover, DME and NO adsorption caused similar consumption patterns of OH-groups at 3792 and 3772 cm^{-1}, which indicate a competition for the same adsorption sites. Another explanation for the higher CO_2(/N_2O) and CO/N_2 formation is the larger number of possible reactions that may occur in the DME-TPR with NO compared with the DME-TPD. Assuming that reactions occur, then it is likely that some methyl groups combine with NO_x species forming nitromethane (CH_3—NO_2), which in turn has been reported to form the observed formohydroxamic acid (CHO—N(H)OH) between 100 and 150 °C [13,37]. Between 150 and 200 °C, only small desorption peaks of other species than DME were observed in the gas phase. The tail of the DME desorption peak coincides with the disappearance of the methoxy band at 1460 and 1473 cm^{-1}, indicating its depletion. The released surface sites may facilitate a rearrangement of the already adsorbed species during which formohydroxamic acid species disappeared, and formaldehyde-like species, formates, isocyanates and nitrates accumulate on the surface as illustrated in Scheme 1. At around 300 °C, desorption peaks of CO_2(/N_2O), CH_4, CO/N_2 and H_2 appeared in the gas phase, while isocyanate and methyl nitrite or nitrosoaldehyde dianion species disappeared and formate species accumulated on the surface. Compared to the DME-TPD, the ratios of CH_4 to CO_2(/N_2O) and H_2 to CO/N_2 decreased in the presence of NO. In terms of mass balance, it is not surprising that a decrease in CH_4 formation coincides with an increase in CO and H_2. Again, the simultaneous formation of CO_2 and CH_4 is explained by the formation of formate species on the surface. The different ratios of the observed species indicate additional reactions in the presence of NO. The reaction of isocyanates with water forms NH_3 and CO_2 [11,12,15,43,44]. The formed ammonia may react with nitrites, forming ammonium nitrites and finally N_2 and water [45], which was detected in increasing amounts above 400 °C. It is thus likely that the increase of the m/z = 28 signal between 300 and 400 °C is partly attributed to the formation of N_2. Except for water, the detected species at 400 °C are similar to the DME-TPD and can be explained by the decomposition of formates.

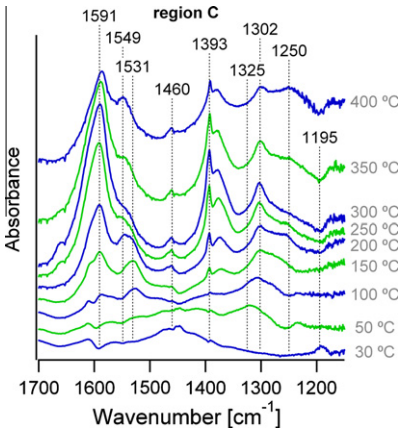

Fig. 6. DRIFTS spectra of γ-alumina samples with pre-adsorbed methanol during temperature-programmed reaction in a flow of 500 ppm NO in Ar.

The DRIFTS spectra of the methanol-TPR in the presence of NO are presented in Fig. 6. The lowermost spectrum is the spectrum of adsorbed methanol at 30 °C, similar to that in Fig. 3. When increasing the temperature, formaldehyde-like species were observed from 150 °C. Besides the assigned features from the methanol-TPD, a broad band at 1325 cm^{-1}, which is assigned to nitrites [46], appeared at 50 °C. Moreover, a band at 1531 cm^{-1}, assigned to formohydroxamic acid (CHO—N(H)OH), appeared at 100 °C and disappeared at 200 °C. At even higher temperatures, bands around 1591, 1549, 1302 and 1250 cm^{-1} appeared, all of which can be assigned to different vibrations of nitrates and possibly nitrites (see Table 3). No formation of isocyanates was detected.

Combining the observations from the DRIFTS measurements and the gas composition of the desorbed species shows that increasing the temperature in the presence of NO leads to desorption of molecularly adsorbed methanol and adsorption of some NO as nitrites. Similar to the DME-TPR with NO, formohydroxamic acid (CHO—N(H)OH) was observed between 100 °C and 200 °C. The reactions proceeding on the alumina surface appear thus to be quite similar during the DME- and methanol-TPR with NO. However, no isocyanates species were detected in the methanol-TPR. It is likely that the higher amount of water, available during methanol-TPR, promotes the reactions of the isocyanates, preventing their accumulation on the surface and thus their detection. Moreover, the higher amount of oxygen available on the surface leads to the formation of more nitrates than in the DME-TPR.

3.3. Reaction of adsorbed surface species with NO_2

In the DME-TPR with NO_2 presented in Fig. 7a, a similar DME desorption peak was observed as in the previous experiments. At 170 °C, desorption peaks of NO (not shown), CO_2(/N_2O) and CO/N_2 appeared and at about 300 °C, further desorption peaks of

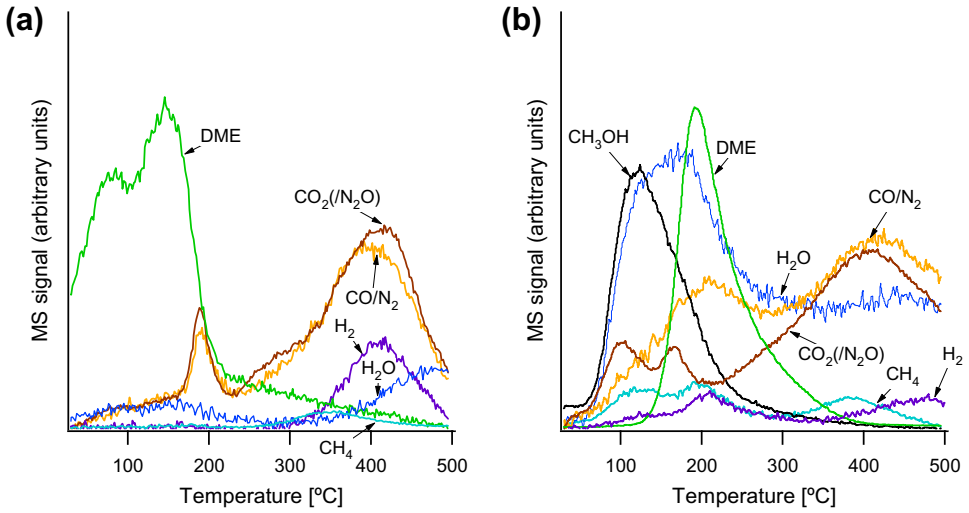

Fig. 7. Temperature-programmed reaction profiles from γ-alumina with pre-adsorbed DME (a) or methanol (b) in a flow of 500 ppm NO_2 in Ar.

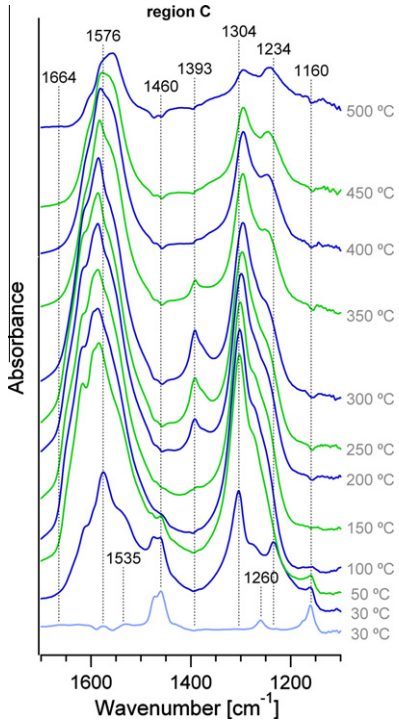

Fig. 8. DRIFTS spectra of γ-alumina samples with pre-adsorbed DME during temperature-programmed reaction in a flow of 500 ppm NO_2 in Ar.

CO_2(/N_2O), H_2, CH_4, CO and/or N_2 were detected. Fig. 7b shows the methanol-TPR in the presence of NO_2. The desorption peaks of methanol and DME were observed also in this experiment. Moreover, high concentrations of water and CO_2 were detected. Similar to the desorption of DME, only a minor amount of CH_4 was detected.

Fig. 8 shows the DRIFTS spectra of the DME-TPR with NO_2, where the lowermost spectrum is the absorption spectrum of DME on alumina without NO_2. The spectra collected in the presence of NO_2 are dominated by large nitrate bands, which hinders the detection and assignment of other bands in their vicinity. The second lowermost spectrum is recorded after 15 min in a flow of 500 ppm NO_2 in Ar at 30 °C and reveals bands of several differently bound nitrates and nitrites around 1576 cm^{-1}, at 1304 cm^{-1} and at 1234 cm^{-1} (see Table 3 for assignments). A shoulder around 1535 cm^{-1} may be due to formohydroxamic acid or to nitrates, since these species were detected in the DME-TPR with NO at 1535 and 1549 cm^{-1}, respectively. However, because of the overlap with the strong nitrate bands an unambiguous assignment is not possible. Increasing the temperature leads to the disappearance of the methoxy species at 100 °C and the accumulation of formate species (1393 cm^{-1}) at 200 °C. At still higher temperatures, the formate species disappeared (400 °C), and the nitrate species decreased (>250 °C) but were still detectable at 500 °C. In contrast to the DME-TPR with NO, neither formaldehyde-like species (2808 cm^{-1}) nor NCO species (2232 and 2249 cm^{-1}) were observed.

The DRIFTS spectra of the methanol-TPR with NO_2 were very similar to those from the DME-TPR with NO_2 and are not presented here. The only differences observed were that no nitrite species at 1234 cm^{-1} were detected and that a shoulder at 1614 cm^{-1}, assigned to nitrates [46–49], was more dominant. The similarities in the two TPR with NO_2 are in contrast to the differences in the results with DME or methanol in the presence of NO, but can be explained by the higher reactivity of NO_2 and the higher oxygen content in NO_2 compared with NO compensating for the differences in oxygen content between DME and methanol.

Below 200 °C, DME desorption due to recombination of methoxy groups was similar for all DME experiments presented here. The desorption peaks of NO, CO_2(/N_2O) and CO/N_2 at around 200 °C appeared at the same temperature where the DME desorption peak rapidly decreased. This indicates that reactions take place on the surface, but no reactions are clearly supported by the DRIFTS spectra in Fig. 8. However, in the DME-TPR with NO, a major rearrangement was observed at the same temperature. It is thus likely that a similar rearrangement takes place in the presence of NO_2 but that the higher reactivity of NO_2 accelerates the reactions with the intermediate species. Because of the faster reactions, no major accumulation of these species is expected, and their detection with DRIFTS prevented. Instead, NO, CO_2(/N_2O) and CO/N_2 desorb into the gas phase. For the desorption peaks at around 300 °C, the same trends are observed, which already have been discussed for the DME-TPR with NO. The relative amounts of CO, H_2O and H_2 were higher, while only a minor amount of CH_4 was formed, which has been explained by more available oxygen. In the methanol-TPR with NO_2, the oxygen available is still higher, explaining the high amounts of formed water and CO_2.

In the presence of oxygen, similar results as in the absence of O_2 are obtained for the TPR studies in the presence of NO or NO_2 in the

gas phase. The CO_2 formation peak at about 400 °C, however, is larger and shifted to somewhat lower temperatures. Moreover, between 30 and about 60 °C a CO_2 peak is observed, while the DME desorption peak is lower in this temperature interval. The DRIFTS spectra obtained during the TPR in the presence of NO and O_2 show the same features as the one of the TPR in the absence of O_2. However, the bands due to nitrates are considerably larger and are observable on the catalyst surface even at 500 °C.

In this study, surface species formed from the absorption of DME and methanol on γ-Al_2O_3 are discussed as well as species that occur in the presence of NO_x. These species are isocyanates and formohydroxamic acid. Since isocyanates are widely discussed as key intermediates in HC-SCR over Ag/Al_2O_3 and formohydroxamic acid is a possible precursor for isocyanate, it appears reasonable to assume that there are strong similarities in the reaction mechanism between HC-SCR over Ag/Al_2O_3 and DME- or methanol-SCR over γ-Al_2O_3. However, since silver is crucial for HC-SCR it appears reasonable that silver activates or partially oxidizes the hydrocarbons. During DME- or methanol-SCR, the reducing agent is obviously activated through another pathway. Formohydroxamic acid and isocyanates appear to be important intermediates in both reaction mechanisms.

4. Conclusions

Adsorption of DME or methanol on a γ-Al_2O_3 catalyst at room temperature results in the formation of water, methoxy groups and, for methanol adsorption, in molecularly adsorbed methanol on the surface. When raising the temperature to 100 °C, DME or methanol desorbs from the surface, depending on the previously adsorbed compound. Between 100 and 200 °C, DME is formed during a rearrangement of surface species, which also results in the formation of a formaldehyde-like species. The presence of NO or NO_2 presumably leads to the combination of some methyl groups with NO_x species forming nitromethane (CH_3-NO_2), as supported by the subsequent formation of formohydroxamic acid (CHO—N(-H)OH) observed in the DME-TPR with NO. At around 200 °C, the DME desorption ceases and the surface species rearrange again. Isocyanates are formed and either accumulate on the surface as in the case of DME-TPR with NO or continue reacting to form NO, CO_2(/N_2O) and CO/N_2 in the case with NO_2 present or in the methanol-TPR. At around 300 °C, formates, CO_2 and CH_4 form from formaldehyde-like species. The largest amount of CH_4 is formed in the TPD with Ar. Its formation is lower in the TPR with NO and lower still in the TPR with NO_2 where larger amounts of CO, H_2 and water are formed instead since more oxygen is available from the NO_2. In the experiments with methanol, the higher oxygen content of two methanol molecules compared with one DME molecule leads to the formation of more water, CO and CO_2 compared with the same experiments with DME. At still higher temperatures, formates decompose to CO and H_2. Some of the observed surface species such as isocyanates and formohydroxamic acid have previously been observed during HC-SCR over Ag/Al_2O_3 catalysts [13], and isocyanates are frequently discussed as key intermediate for HC-SCR over Ag/Al_2O_3 [6–8,10,13,15,48,50]. Therefore, we suggest that the reaction mechanism for DME-SCR over Al_2O_3 is similar to that proposed for hydrocarbons over Ag/Al_2O_3, except for the activation step leading to the formation of formohydroxamic acid in the former mechanism.

Acknowledgments

This work was performed within the Competence Centre for Catalysis, which is hosted by Chalmers University of Technology and financially supported by the Swedish Energy Agency and the member companies: AB Volvo, Volvo Car Corporation, Scania CV AB, Saab Automobile Powertrain AB, Haldor Topsøe A/S and the Swedish Space Corporation. A.E.C. Palmqvist gratefully acknowledges support from the Swedish Research Council (VR) for a Senior Researcher position.

Appendix A. Supplementary material

Supplementary data associated with this article can be found, in the online version, at doi:10.1016/j.jcat.2010.10.004.

References

[1] P. Ahlvik, Å. Brandberg, Well-to-wheel Efficiency for Alternative Fuels from Natural Gas and Biomass, first ed., Swedish National Road Administration, Borlänge, 2001. pp. 1–121. <http://www.vv.se/filer/publikationer/2001-85.pdf> (accessed 10.11.07)..
[2] R. Edwards, J.-F. Larivé, V. Mahieu, R. Rouveirolles, Well-to-wheels Analysis of Future Automotive Fuels and Powertrains in the European Context, European Commission Joint Research Centre, 2006. <http://www.jrc.cec.eu.int/wtw.html> (accessed 09.07.07).
[3] S. Erkfeldt, A.E.C. Palmqvist, E. Jobson, Top. Catal. 42–43 (2007) 149–152.
[4] K. Masuda, K. Tsujimura, K. Shinoda, T. Kato, Appl. Catal. B: Environ. 8 (1996) 33–40.
[5] S. Tamm, H.H. Ingelsten, M. Skoglundh, A.E.C. Palmqvist, Top. Catal. 52 (2009) 1813–1816.
[6] R. Burch, J.P. Breen, F.C. Meunier, Appl. Catal. B: Environ. 39 (2002) 283–303.
[7] K. Shimizu, J. Shibata, H. Yoshida, A. Satsuma, T. Hattori, Appl. Catal. B: Environ. 30 (2001) 151–162.
[8] S. Tamm, H.H. Ingelsten, A.E.C. Palmqvist, J. Catal. 255 (2008) 304–312.
[9] A. Iglesias-Juez, A.B. Hungria, A. Martinez-Arias, A. Fuerte, M. Fernandez-Garcia, J.A. Anderson, J.C. Conesa, J. Soria, J. Catal. 217 (2003) 310–323.
[10] S. Sumiya, H. He, A. Abe, N. Takezawa, K. Yoshida, J. Chem. Soc. Faraday Trans. 94 (1998) 2217–2219.
[11] N.W. Cant, I.O.Y. Liu, Catal. Today 63 (2000) 133–146.
[12] T. Nanba, A. Obuchi, Y. Sugiura, C. Kouno, J. Uchisawa, S. Kushiyama, J. Catal. 211 (2002) 53–63.
[13] V. Zuzaniuk, F.C. Meunier, J.R.H. Ross, J. Catal. 202 (2001) 340–353.
[14] A.D. Cowan, N.W. Cant, B.S. Haynes, P.F. Nelson, J. Catal. 176 (1998) 329–343.
[15] N. Bion, J. Saussey, M. Haneda, M. Daturi, J. Catal. 217 (2003) 47–58.
[16] S. Kameoka, T. Chafik, Y. Ukisu, T. Miyadera, Catal. Lett. 51 (1998) 11.
[17] M. Alam, O. Fujita, K. Ito, Proc. Inst. Mech. Eng. Part A: J. Power Energy 218 (2004) 89–95.
[18] S.G. Masters, D. Chadwick, Appl. Catal. B: Environ. 23 (1999) 235–246.
[19] J.W. Park, C. Potvin, G. Djega-Mariadassou, Top. Catal. 42–43 (2007) 259–262.
[20] S. Tamm, H.H. Ingelsten, M. Skoglundh, A.E.C. Palmqvist, Appl. Catal. B: Environ. 91 (2009) 234–241.
[21] E. Ozensoy, D. Herling, J. Szanyi, Catal. Today 136 (2008) 46–54.
[22] T. Matsushima, J.M. White, J. Catal. 44 (1976) 183–196.
[23] A.R. McInroy, D.T. Lundie, J.M. Winfield, C.C. Dudman, P. Jones, D. Lennon, Langmuir 21 (2005) 11092–11098.
[24] J.G. Chen, P. Basu, T.H. Ballinger, J.T. Yates, Langmuir 5 (1989) 352–356.
[25] H. Knözinger, P. Ratnasamy, Catal. Rev. Sci. Eng. 17 (1978) 31–70.
[26] M. Digne, P. Sautet, P. Raybaud, P. Euzen, H. Toulhoat, J. Catal. 226 (2004) 54–68.
[27] T.H. Ballinger, J.T. Yates, Langmuir 7 (1991) 3041–3045.
[28] A. Martinez-Arias, M. Fernandez-Garcia, A. Iglesias-Juez, J.A. Anderson, J.C. Conesa, J. Soria, Appl. Catal. B: Environ. 28 (2000) 29–41.
[29] P.F. Rossi, G. Busca, V. Lorenzelli, Z. Phys. Chem. N. F. 149 (1986) 99–111.
[30] G. Busca, P.F. Rossi, V. Lorenzelli, M. Benaissa, J. Travert, J.C. Lavalley, J. Phys. Chem. 89 (1985) 5433–5439.
[31] V.A. Matyshak, L.A. Berezina, O.N. Sil'chenkova, V.F. Tret'yakov, G.I. Lin, A.Y. Rozovskii, Kinet. Catal. 50 (2009) 111–121.
[32] H.W. Gao, T.X. Yan, J. Mol. Struct. 889 (2008) 191–196.
[33] G. Busca, J. Lamotte, J.C. Lavalley, V. Lorenzelli, J. Am. Chem. Soc. 109 (1987) 5197–5202.
[34] J.T. Yates, R.R. Cavanagh, J. Catal. 74 (1982) 97–109.
[35] G. Busca, Catal. Today 27 (1996) 457–496.
[36] M. Yamaguchi, J. Chem. Soc. Faraday Trans. 93 (1997) 3581–3586.
[37] Y.H. Yeom, B. Wen, W.M.H. Sachtler, E. Weitz, J. Phys. Chem. B 108 (2004) 5386–5404.
[38] F.C. Meunier, J.P. Breen, V. Zuzaniuk, M. Olsson, J.R.H. Ross, J. Catal. 187 (1999) 493–505.
[39] V.A. Sadykov, V.V. Lunin, V.A. Matyshak, E.A. Paukshtis, A.Y. Rozovskii, N.N. Bulgakov, J.R.H. Ross, Kinet. Catal. 44 (2003) 379–400.
[40] T. Tanaka, T. Okuhara, M. Misono, Appl. Catal. B: Environ. 4 (1994) L1–L9.
[41] Y. Ukisu, S. Sato, G. Muramatsu, K. Yoshida, Catal. Lett. 11 (1991) 177–181.
[42] M.L. Unland, J. Phys. Chem. 77 (1973) 1952–1956.
[43] A. Obuchi, C. Wögerbauer, R. Köppel, A. Baiker, Appl. Catal. A 19 (1998) 9–22.
[44] X.L. Zhang, H. He, Z.C. Ma, Chem. Commun. 8 (2007) 187–192.
[45] Y.H. Yeom, J. Henao, M.J. Li, W.M.H. Sachtler, E. Weitz, J. Catal. 231 (2005) 181–193.

[46] K.I. Hadjiivanov, Catal. Rev. Sci. Eng. 42 (2000) 71–144.
[47] K. Shimizu, H. Kawabata, A. Satsuma, T. Hattori, J. Phys. Chem. B 103 (1999) 5240–5245.
[48] H. He, Y.B. Yu, Catal. Today 100 (2005) 37–47.
[49] S. Kameoka, Y. Ukisu, T. Miyadera, Phys. Chem. Chem. Phys. 2 (2000) 367–372.
[50] S. Kameoka, T. Chafik, Y. Ukisu, T. Miyadera, Catal. Lett. 55 (1998) 211–215.
[51] R. Burch, J.P. Breen, C.J. Hill, B. Krutzsch, B. Konrad, E. Jobson, L. Cider, K. Eränen, F. Klingstedt, L.E. Lindfors, Top. Catal. 30–31 (2004) 19–25.
[52] P. Sazama, L. Capek, H. Drobna, Z. Sobalik, J. Dedecek, K. Arve, B. Wichterlová, J. Catal. 232 (2005) 302–317.
[53] B. Wichterlová, P. Sazama, J.P. Breen, R. Burch, C.J. Hill, L. Čapek, Z. Sobalík, J. Catal. 235 (2005) 195–200.
[54] A. Satsuma, K. Shimizu, Progr. Energy Combust. Sci. 29 (2003) 71–84.
[55] N. Bion, J. Saussey, C. Hedouin, T. Seguelong, M. Daturi, Phys. Chem. Chem. Phys. 3 (2001) 4811–4816.
[56] F.C. Meunier, V. Zuzaniuk, J.P. Breen, M. Olsson, J.R.H. Ross, Catal. Today 59 (2000) 287–304.
[57] J. Wang, H. He, Q.C. Feng, Y.B. Yu, K. Yoshida, Catal. Today 93–95 (2004) 783–789.